Resonant two-photon ionization spectroscopy of NiC

Dale J. Brugh and Michael D. Morse
University of Utah, Salt Lake City, Utah 84112

(Received 2 August 2002; accepted 16 September 2002)

A spectroscopic investigation of jet-cooled diatomic NiC has revealed a complex pattern of vibronic levels in the wave number range from 21 700 to 27 000 cm^{-1}. Of the more than 50 vibronic bands observed, 31 have been rotationally resolved and analyzed. All are $\Omega' = 0^+ \leftarrow \Omega'' = 0^+$ transitions, consistent with the calculated $^1\Sigma^+$ ground state of this molecule. Through the observation of vibrational hot bands in the spectra, these measurements have established that $\omega_e'' = 875.155\ cm^{-1}$, $\omega_e x_e = 5.38\ cm^{-1}$, $B_e = 0.640\,38(14)\ cm^{-1}$, $\alpha_e = 0.004\,44(36)\ cm^{-1}$, and $r_e = 1.6273(2)$ Å for $^{58}Ni^{12}C$. Several possible electronic band systems are observed, but the identification of these is hampered by extensive perturbations among the excited states. The observation of long-lived vibronic states as far to the blue as 26 951 cm^{-1} indicates that $D_0(NiC) \geqslant 3.34$ eV, and the ionization energy of NiC has been determined to fall in the range $IE(NiC) = 8.73 \pm 0.39$ eV. A discussion of these results, in the context of work on other $3d$ transition metal carbides is also presented. © *2002 American Institute of Physics.* [DOI: 10.1063/1.1519257]

I. INTRODUCTION

The transition metal carbides provide an interesting and important set of diatomic molecules for experimental and theoretical study, because of the significance of the transition metal–carbon bond in homogeneous and heterogeneous catalysis, biological processes, and organometallic chemistry. In addition, it is likely that some transition metal monocarbides (particularly those of the $3d$ period) may be found in the circumstellar envelopes of carbon-rich stars,[1,2] making these species of interest to the astrophysical community as well. For these reasons we have investigated a number of the diatomic transition metal carbides over the past five years.[3–8] In this article we present the results of spectroscopic studies of diatomic NiC.

Among the transition metal carbides, the $4d$ series is by far the most completely studied. Experimental studies of the spectra of YC,[9] ZrC,[10] NbC,[11] MoC,[4,7] RuC,[5,7,12–14] RhC,[12–15] and PdC[6,7] have been published, and theoretical investigations have been reported for YC,[16] NbC,[11] MoC,[17] TcC,[18] RuC,[19,20] RhC,[21,22] and PdC.[23–27] Because of this extensive amount of work, the electronic structure and chemical bonding trends in this group of molecules are reasonably well-known. In contrast, experimental data on the $5d$ transition metal carbides is severely limited, with spectra available only for WC,[8,28] IrC,[29,30] and PtC.[31–38] Likewise, rather few theoretical studies of the $5d$ transition metal carbides have been reported, with published reports on the diatomics TaC,[39] WC,[40] OsC,[41] IrC,[42] and PtC[43] only. The $5d$ transition metal carbides represent a particular challenge to theoretical chemistry because of the simultaneous importance of relativistic, electron correlation, and spin–orbit effects. Experimental data for the $3d$ transition metal carbides is similarly limited, with published analyses only available for FeC,[3,44–48] CoC,[1,49,50] and NiC.[1] In the case of the $3d$ transition metal carbides a rather large number of theoretical calculations have been reported, however, on ScC,[51] TiC,[52–55] VC,[56,57] CrC,[58–60] FeC,[61–64] and NiC.[65–68] Although relativistic effects are considerably less important in these molecules than in the $4d$ and $5d$ series, the compact nature of the $3d$ orbitals makes electron correlation a more significant problem in the $3d$ series than in either the $4d$ or $5d$ series.

Among the $3d$ transition metal carbides, NiC is the third of the $3d$ transition metal monocarbides to be spectroscopically investigated in the gas phase. The first was FeC, with optical spectra reported to the blue of 500 nm by Balfour *et al.*,[44] and to the red of 500 nm by this laboratory.[3] Since these initial studies, additional absorption, stimulated emission pumping, and laser-induced fluorescence (LIF) studies have been highly successful in sorting out the electronic states of FeC.[46–48] In addition, the first millimeter wave study of a transition metal carbide was carried out on FeC in 1996,[45] establishing the rotational constants to high precision. As a result of these studies, the ground state of FeC is firmly established as $^3\Delta_3$, deriving from a $7\sigma^2 8\sigma^2 3\pi^4 1\delta^3 9\sigma^1$ molecular orbital configuration. The low-lying $^1\Delta$ state deriving from the same configuration has also been located and identified.[48] Next to be investigated was CoC, for which LIF studies were reported in 1995[49] and 1997.[50] These investigations demonstrated that the ground state of CoC is $7\sigma^2 8\sigma^2 3\pi^4 1\delta^4 9\sigma^1$, $^2\Sigma^+$, and identified a $7\sigma^2 8\sigma^2 3\pi^4 1\delta^3 9\sigma^2$, $^2\Delta_{5/2}$ state lying only 221 cm^{-1} above the ground state. Millimeter wave spectra of CoC and NiC have recently been recorded and analyzed as well, providing the ground-state rotational constants to high accuracy.[1]

To our knowledge, no published optical spectra exist for diatomic NiC. In unpublished work, however, Balfour, Qian, and Zhou have collected an LIF spectrum of the products resulting from laser ablation of a Ni target in the throat of a helium supersonic expansion seeded with methane.[69] The spectrum is complicated and congested, but some of the transitions are now known to be due to NiC based on the work presented here. The present study provides the first analysis of the optical spectra of NiC to be presented in the literature.

The first theoretical calculation on NiC was reported in 1982 by Kitaura, Morokuma, and Csizmadia.[65] These authors used generalized valence bond methods to calculate the potential energy curve of an assumed $^1\Sigma^+$ ground state deriving from Ni ($3d^9 4s^1$, ^{3}D) + C ($2s^2 2p^2$, ^{3}P) at various internuclear separations. The resulting value of the bond length, $r_0 = 1.8$ Å, is rather long compared to measured values, and no attempt was made to confirm that the ground state is truly of $^1\Sigma^+$ symmetry. By modern standards, this calculation may be considered to be rather primitive. In 1989, Shim and Gingerich conducted *ab initio* calculations in which several electronic states were considered, and the ground state was predicted to be a $^1\Sigma^+$ term.[67] The bonding in NiC was found to be quite polar, with substantial electron transfer from the Ni atom to the C ligand. At a Ni–C separation of 1.9 Å, the atomic charge on Ni becomes +0.40e. As a result, simple electrostatic interactions between the Ni and C atoms are expected to contribute substantially to the bonding in this molecule. Indeed, this study concludes that the low lying states of NiC all derive from the various angular momentum couplings of a $3d^8 4s^1$, ^{4}F Ni^+ ion with a $2s^2 2p^3$, ^{4}S C^- ion. In a 1999 study Shim and Gingerich have reinvestigated the NiC molecule using multireference configuration interaction calculations (MRCI) methods, and have again found that the ground state is $^1\Sigma^+$, but this state is now separated from a dense manifold of excited states by 6465 cm^{-1}.[68] The calculated values of $r_e = 1.621$ Å and $\omega_e = 874$ cm^{-1} are in excellent agreement with results obtained from the present study, provided below.

Section II of this paper provides a brief review of the experimental methods employed in these studies, while the results obtained are presented in Sec. III. These results are discussed and placed in context in Sec. IV, and Sec. V then concludes the paper with a summary of our most important findings.

II. EXPERIMENT

The resonant two-photon ionization (R2PI) spectroscopy of NiC was carried out using an instrument that has been previously described,[70] and which was used in studies of the other metal carbides FeC,[3] MoC,[4] RuC,[5] PdC,[6] and WC.[8] Diatomic NiC was produced by laser ablation (532 nm, 1 mJ/pulse) of a pure Ni sample in the throat of a supersonic expansion of helium seeded with 3% CH_4. A backing pressure of 80–100 psig was found to be most efficient for formation of the molecule in its ground vibronic state. Hot bands originating from $v = 1$ and 2 were efficiently observed under conditions of lower backing pressure (40–60 psig), coupled with a reduction in the pulsed nozzle operating voltage, which also reduced the carrier gas pressure over the nickel metal target.

To conduct the low resolution (0.6 cm^{-1}) survey work for this molecule, a Molectron dye laser was pumped by the third harmonic of a Nd:YAG laser to produce the necessary excitation radiation. The dyes used to generate the spectroscopic photons for survey work from 19 200 to 24 000 cm^{-1} included Coumarin 500, 480, 460, 440, and Stilbene 420. The range from 24 000 to 27 000 cm^{-1} was examined using Exalite dyes 411, 404, 398, 389, and 376 dissolved in p-dioxane. Following irradiation with the tunable dye laser light, the molecular beam was exposed to a pulse of ArF excimer radiation at 6.42 eV. Excited state lifetimes were measured by varying the delay between the excitation and the ionization laser pulses, and fitting the resulting ion signal curve to an exponential decay model. By this method, the 1/e decay times, τ, were extracted for many of the excited vibronic levels probed.

Rotationally resolved work was carried out by narrowing the output linewidth of the dye laser to 0.04 cm^{-1} by inserting an air spaced étalon into the oscillator cavity. The output wave number of the dye laser was then scanned over a range of about 15 cm^{-1} by pressurizing the cavity from about 10 Torr to atmospheric pressure with Freon-12 (CF_2Cl_2, DuPont). For bands lying between 19 200 and 23 800 cm^{-1}, linearization of the spectrum was achieved by collecting the transmission fringes of a separate monitor étalon, and calibration of the spectrum was accomplished by simultaneously collecting the absorption spectrum of $^{130}Te_2$ at 510 °C. Comparison with the atlas of Cariou and Luc[71,72] then allowed absolute line positions to be obtained for the molecular spectrum of NiC.

Above 23 800 cm^{-1} this calibration method could not be employed, because the Te_2 atlas does not continue beyond this point. Therefore, the dye laser was operated on the near-infrared LDS laser dyes, and the output dye laser radiation was frequency doubled to generate wave numbers in the range of 23 800–27 000 cm^{-1}. The infrared radiation was used for calibration by recording the absorption spectrum of a gaseous I_2 sample heated to either 500 °C or 790 °C, while the second harmonic radiation was used to excite the NiC molecule. The I_2 absorption spectrum was then compared to the atlas of Gerstenkorn, Verges, and Chevillard[73] to obtain a precise spectral calibration. In either calibration method, a correction for the Doppler shift caused by the motion of the NiC molecules toward the excitation source was included. It is believed that the wave numbers of all rotationally resolved features reported in this work are accurate to within ±0.02 cm^{-1}.

III. RESULTS

A. General features

The low resolution survey spectrum of NiC yielded nearly 50 bands. The spectrum begins at ~21 750 cm^{-1} where an intense transition was discovered. To the blue of this value, the spectrum remains fairly sparse for the next 2000 cm^{-1}. It consists of a number of very weak features and a few moderately intense ones. From 23 700 cm^{-1} to the limit of this study at 27 000 cm^{-1}, the spectrum is considerably more congested and much more intense, as may be seen in Fig. 1. Of the observed transitions, 31 were selected for investigation at higher resolution in the hope of making sense of the confusing array of vibronic transitions. All of the rotationally resolved bands was found to lack a Q-branch, proving that the Ω values of both the upper and lower states were zero. Although this differed from what was found for MoC,[4] where all of the bands examined were of $\Omega' = 1 \leftarrow \Omega'' = 0$ symmetry, the lack of variety was equally exasper-

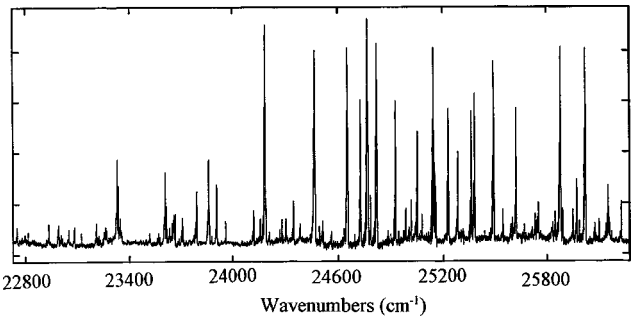

FIG. 1. Low resolution (0.5 cm^{-1}) spectrum of $^{58}Ni^{12}C$, over the range 22 800–26 300 cm^{-1}.

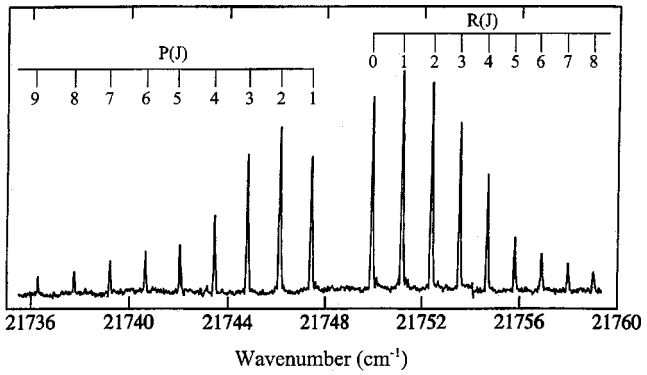

FIG. 2. Rotationally resolved (0.03 cm^{-1}) scan over the 0–0 band of the $[21.7]0^+ - X\,^1\Sigma^+$ system of $^{58}Ni^{12}C$, near 21749 cm^{-1}. The absence of a Q branch demonstrates that this is an $\Omega = 0 \leftarrow \Omega = 0$ transition.

ating in the case of NiC. The fact that all of the observed states of NiC have $\Omega = 0$ made it much more difficult to group the observed bands into electronic band systems. Fortunately, in the present investigation we were able to identify hot bands originating from $v'' = 1$ and 2, allowing accurate values of B_e, α_e, r_e, ω_e, and $\omega_e x_e$ to be determined for the ground state.

Initial attempts to find vibronic progressions in the spectrum of NiC were made by seeking sets of bands that were nearly equally spaced, according to the harmonic oscillator assumption. This procedure, as in our previous study of MoC,[4] failed to yield any candidate band systems. To identify potential band systems, another method was used. In this procedure, the isotope shift of a band, calculated as $\Delta\nu \equiv \nu(^{58}Ni^{12}C) - \nu(^{60}Ni^{12}C)$, is plotted as a function of the band origin for the $^{58}Ni^{12}C$ isotopomer, $\nu(^{58}Ni^{12}C)$. Assuming that the anharmonicity may be ignored, the points corresponding to bands belonging to the same electronic band system are expected to fall on a line of predetermined slope. Thus, by spreading the data out into two dimensions, and searching for groups of bands that follow the expected relationship, it may become possible to identify bands which belong to the same band system. This procedure was helpful in our previous study of MoC.[4]

To demonstrate that the isotope shifts within a band system are a linear function of the band origin, we employ the standard formula for a molecule that follows the harmonic oscillator model:

$$\nu(^{58}Ni^{12}C) = T_e + \omega_e'(v' + \tfrac{1}{2}) - \omega_e''(v'' + \tfrac{1}{2}). \tag{3.1}$$

The expression for the transition energy of the $^{60}Ni^{12}C$ isotopic modification, $\nu(^{60}Ni^{12}C)$, is given by

$$\nu(^{60}Ni^{12}C) = T_e + \rho\,\omega_e'(v' + \tfrac{1}{2}) - \rho\,\omega_e''(v'' + \tfrac{1}{2}), \tag{3.2}$$

where ω_e' and ω_e'' still pertain to the $^{58}Ni^{12}C$ isotopomer, and ρ is given by[74]

$$\rho = \sqrt{\frac{\mu(^{58}Ni^{12}C)}{\mu(^{60}Ni^{12}C)}}. \tag{3.3}$$

Subtracting Eq. (3.1) from (3.2) then gives

$$\Delta\nu \equiv \nu(^{60}Ni^{12}C) - \nu(^{58}Ni^{12}C) = (\rho - 1)[\nu(^{58}Ni^{12}C) - T_e]. \tag{3.4}$$

Thus, a plot of the isotope shift, $\Delta\nu$, as a function of $\nu(^{58}Ni^{12}C)$ for all the transitions belonging to the same band system is expected to yield a line of slope $\rho - 1$. Further, the line should cross the ν axis at the value $\nu = T_e$.

Using the accurate atomic masses provided by DeBierre *et al.*,[75] ρ is calculated as $\rho = 0.997\,137$, giving $\rho - 1 = -0.002\,861$. A search for data points on the $\Delta\nu$ versus ν plot that could be connected using a line of slope $-0.002\,86$ led to the discovery of four such lines with slopes very near the calculated value. The close agreement of these slopes with one another and with the expected value was of great help in identifying four band systems in the spectra of NiC. These are discussed in more detail below.

All of the rotationally resolved bands investigated in this study were readily fitted to the simple formula

$$\nu = \nu_0 + B'J'(J' + 1) - B''J''(J'' + 1), \tag{3.5}$$

which is valid for $\Omega' = 0 \leftarrow \Omega'' = 0$ bands, provided perturbations by other states are insignificant and centrifugal distortion is negligible. Fits of the line positions for each band to Eq. (3.5) provided fitted values for ν_0, B', and B'' for each band. On average, only about ten lines were measured in each band, although for some bands as many as 19 lines were recorded.

B. The $[21.7]\Omega = 0^+$ state

A lone vibronic transition of NiC occurs near 21 750 cm^{-1}, well isolated from everything else in the spectrum. The rotationally resolved spectrum of this band is displayed in Fig. 2. The band clearly possesses only *P* and *R* branches, indicating that it is an $\Omega' = 0 \leftarrow \Omega'' = 0$ transition. Based on the theoretical calculations described in Sec. I, it may be assumed that the ground state is of $^1\Sigma^+$ symmetry.[65–68] As a result, only transitions to upper states with $\Omega' = 0^+$ or 1 are allowed under electric dipole selection rules. Accordingly, the upper state of the band displayed in Fig. 2 must have $\Omega' = 0^+$. Further, the *P* and *R* branches fan out symmetrically on either side of the band origin, indicating that the rotational constants B' and B'' are nearly identical. When this spectrum is fit to Eq. (3.5), the extracted spectroscopic parameters are $B'' = 0.637\,599(82)$ cm^{-1}, $B' = 0.624\,640(88)$ cm^{-1}, and $\nu_0 = 21\,748.6942(15)$ cm^{-1}.

TABLE I. Identified NiC band systems.[a]

State	$v'-v''$	ν_0 (cm^{-1})[b]	B'' (cm^{-1})[b]	B' (cm^{-1})[b]	$\Delta\nu_0$ (cm^{-1})[c]	τ(ns)
$[21.7]\Omega=0^+$	0–0	21 748.6943(15)	0.637 648[d]	0.624 689(33)	+0.0111(32)	560(65)
$[23.8]\Omega=0^+$	1–2	22 738.50(50)	⋯	⋯	+2.60(50)[e]	
	1–1	23 595.1482(20)	0.632 31(17)	0.515 17(11)	−0.0083(52)	78(10)
	0–0	23 848.9133(53)	0.637 648[d]	0.527 45(16)	−1.3512(65)	314(15)
	1–0	24 459.5499(50)	0.637 648[d]	0.514 41(14)	−2.4567(57)	95(2)
	2–0	25 222.1387(37)	0.637 648[d]	0.525 73(27)	−4.4199(49)	256(17)
	3–0	25 868.9024(44)	0.637 648[d]	0.506 00(13)	−5.4995(94)	107(2)
	4–0	26 399.9264(50)	0.637 648[d]	0.502 87(22)	−6.9735(84)	131(2)
$[24.2]\Omega=0^+$	0–2	22 463.7750(49)	0.624 93(88)	0.502 34(61)	+4.3118(62)	
	0–1	23 317.4038(10)	0.632 31(17)	0.503 07(11)	+1.9570(23)	96(2)
	1–1	23 896.3264(34)	0.632 31(17)	0.507 82(22)	+0.7060(62)	73(2)
	0–0	24 181.7969(24)	0.637 648[d]	0.503 51(32)	−0.4834(30)	95(6)
	1–0	24 760.7020(44)	0.637 648[d]	0.509 11(31)	−1.7182(63)	68(2)
$[24.6]\Omega=0^+$	0–1	23 780.21(50)	⋯	⋯	+1.30(50)[e]	
	0–0	24 643.8517(67)	0.637 648[d]	0.493 97(23)	−1.0764(69)	186(18)
$[24.8]\Omega=0^+$	0–1	23 947.05(50)	⋯	⋯	+2.08(50)[e]	
	0–0	24 810.2459(44)	0.637 648[d]	0.474 98(22)	−0.5594(69)	214(3)

[a]Error limits are given in parentheses in units of the last reported digits, and represent 1σ in the fitted quantity.
[b]Measured for $^{58}Ni^{12}C$.
[c]The isotope shift, $\Delta\nu_0$, is defined as $\nu_0(^{60}Ni^{12}C)-\nu_0(^{58}Ni^{12}C)$.
[d]Held fixed at the value measured in millimeter wave experiments (Ref. 1).
[e]Measured in low resolution.

The 1σ error limits, in units of the last two decimal places, are given in parentheses here and throughout the remainder of this paper. This fitted value of B'' is in excellent agreement with the millimeter wave measurement, $B''_0 = 0.637\,648\,3(4)\ cm^{-1}$,[1] demonstrating that the transition does originate from the ground state.

The isotope shift $\Delta\nu_0$ for this band is just 0.0107(29) cm^{-1}. Such a small value for $\Delta\nu_0$ is indicative of an origin band. Accordingly, the 21 750 cm^{-1} band is assigned as the origin band of the $[21.7]\Omega=0^+\leftarrow X\,^1\Sigma^+$ system. The fact that the rotational constant (and consequently, the bond length) changes by so little upon excitation explains why no other members of a progression are observed for this electronic state. Spectroscopic constants for all of the rotationally resolved bands belonging to identified band systems are provided in Table I; fitted constants for bands not belonging to identified band systems are in Table II. A complete listing of the fitted rotational lines, along with fitted spectroscopic constants for all of the rotationally resolved bands is available via the Electronic Physics Auxiliary Publication Service (EPAPS) or through the author (MDM).[76]

To the blue of this band it becomes more difficult to identify individual electronic states. An interval of about 864 cm^{-1} can be found separating five pairs of bands in the next

TABLE II. Spectroscopic constants for NiC bands that do not belong to identified band systems.[a]

v''	ν_0 (cm^{-1})[b]	B'' (cm^{-1})[b]	B' (cm^{-1})[b]	$\Delta\nu_0$ (cm^{-1})[c]	τ(ns)
0	24 718.2240(60)	0.637 648[d]	0.519 46(12)	−3.2743(98)	285(5)
0	24 918.8588(30)	0.637 648[d]	0.516 89(59)	−3.0033(61)	210(18)
0	25 045.6193(49)	0.637 648[d]	0.535 98(45)	−5.0876(59)	273(10)
0	25 138.7230(77)	0.637 648[d]	0.465 89(48)	−1.5901(88)	239(7)
0	25 276.9326(98)	0.637 648[d]	0.469 29(84)	−1.3054(104)	307(30)
0	25 350.2173(67)	0.637 648[d]	0.529 32(36)	−4.0504(82)	122(20)
0	25 369.5183(36)	0.637 648[d]	0.515 23(21)	−3.8624(66)	102(3)
0	25 486.6670(53)	0.637 648[d]	0.509 87(50)	−2.5082(61)	93(2)
0	25 615.8844(80)	0.637 648[d]	0.469 89(14)	−4.0438(90)	302(16)
0	26 012.8886(42)	0.637 648[d]	0.504 10(46)	−5.0393(60)	55(2)
0	26 455.7468(34)	0.637 648[d]	0.459 74(27)	−5.4983(63)	223(3)
0	26 604.3322(67)	0.637 648[d]	0.478 75(30)	−7.8054(121)	206(8)
0	26 702.3966(61)	0.637 648[d]	0.424 92(32)	−9.1140(98)	286(7)
0	26 728.0247(48)	0.637 648[d]	0.431 92(33)	−9.2878(60)	290(2)
0	26 823.2506(44)	0.637 648[d]	0.507 05(27)	−5.4369(77)	115(3)
0	26 929.1515(70)	0.637 648[d]	0.412 84(39)	−6.9973(94)	235(3)
0	26 951.3790(135)	0.637 648[d]	0.485 27(18)	−9.0840(141)	269(11)

[a]Error limits are given in parentheses in units of the last reported digits, and represent 1σ in the fitted quantity. All bands investigated have $\Omega'=0^+$.
[b]Measured for $^{58}Ni^{12}C$.
[c]The isotope shift, $\Delta\nu_0$, is defined as $\nu_0(^{60}Ni^{12}C)-\nu_0(^{58}Ni^{12}C)$.
[d]Held fixed at the value measured in millimeter wave experiments (Ref. 1).

3500 cm^{-1}, and two pairs of bands are separated by about 854 cm^{-1} in this same region, but these are the only hints at order in the vibronic spectrum. These intervals are identified below as vibrational intervals in the $X\,^1\Sigma^+$ ground state corresponding to $\Delta G''_{1/2}$ and $\Delta G''_{3/2}$, respectively.

C. The $[23.8]\Omega=0^+$ state

Three bands with origins near 22 739, 23 595, and 24 460 cm^{-1} possess isotope shifts as a function of frequency that lie along a line with a least squares slope of −0.002 936. This is very close to the expected slope of −0.002 861, making these bands strong candidates for a band system. The first of these bands was not rotationally resolved; its isotope shift was instead measured from low resolution survey scans. The interval between the first two of these bands is 856.65(50) cm^{-1}; the interval between the second two is 864.4017(54) cm^{-1}. This is not the expected pattern for a progression in the excited state vibrational quantum number, v', because it implies a negative value of the anharmonicity, $\omega'_e x'_e$. In addition, the lower state rotational constants for the 23 595 and 24 460 cm^{-1} bands differ significantly, indicating that the two transitions originate from different lower states. Finally, the B'' value of the 24 460 cm^{-1} band equals the millimeter wave value of $B''_0=0.637\,648\,3(4)$ cm^{-1},[1] within the error limits of the present investigation. Accordingly, these three bands are assigned as the $v'-2$, $v'-1$, and $v'-0$ bands of a new band system. The fact that these bands correspond to a progression in the lower state vibrational quantum number, v'', explains why the slope of the line through the $(\nu, \Delta\nu)$ data points matches so closely with the calculated value of $\rho-1$. The vibrational levels of the ground state are presumably unperturbed, such that any set of $v'-v''$ bands terminating on the same value of v' may be expected to adhere to the predictions of Eq. (3.4) quite closely.

Next, it must be decided whether the band near 24 460 cm^{-1} is the 0–0 band of this system. This seems unlikely because of the large isotope shift observed (−2.46 cm^{-1}). It is more likely that the 24 460 cm^{-1} band is the 1–0 band, the 23 595 cm^{-1} band is the 1–1 band, and the 22 739 cm^{-1} band is the 1–2 band. This assignment is supported by the fact that the line drawn through the 1–0, 1–1, and 1–2 data points may be extended, and in so doing it passes close to several other data points which may be assigned as the 0–0, 2–0, 3–0, and 4–0 bands. These occur near 23 849, 25 222, 25 869, and 26 400 cm^{-1}, respectively, and all of these bands have been rotationally resolved. In addition, weaker features are evident in the low-resolution spectrum that correspond to the 0–2, 0–1, 2–2, 3–2, 3–1, 4–2, and 4–1 hot bands. A plot of the measured isotope shifts versus band origin for these features is presented in Fig. 3, along with a line drawn with the theoretical slope of −0.002 861, which serves as a guide for the eye.

While these bands fall close to the theoretical line for isotope shift as a function of band position, this assignment gives upper state levels that are quite erratic in their spacing, with intervals of $\Delta G_{1/2}=611\ cm^{-1}$, $\Delta G_{3/2}=763\ cm^{-1}$, $\Delta G_{5/2}=647\ cm^{-1}$, and $\Delta G_{7/2}=531\ cm^{-1}$. Nevertheless, the average spacing is 638 cm^{-1}, which is a reasonable value for an excited state of a transition metal carbide. In addition, the B'_v values for $v'=0-4$ change in the expected manner, with the exception of the $v'=2$ level, which displays an anomalously large B' value. The excited state lifetimes for these levels also vary considerably, ranging from 95 ns (for $v'=1$) to 314 ns (for $v'=0$). All of these variations suggest that perturbations with nearby states play an important role in the spectroscopy of NiC. Such perturbations are unfortunately turning out to be more the rule than the exception in the spectra of the transition metal carbides.

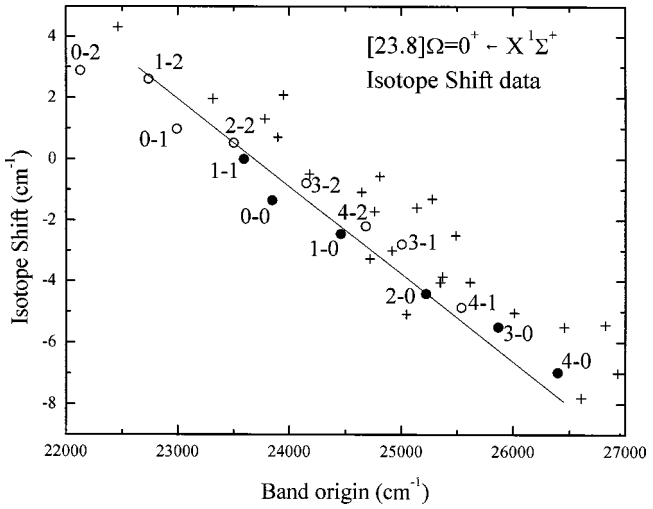

FIG. 3. Measured isotope shifts vs band origin. Bands assigned to the $[23.8]0^+\leftarrow X\,^1\Sigma^+$ system are shown as circles, with solid circles providing isotope shifts measured in high resolution. Open circles provide isotope shifts measured from low resolution scans. Plus signs (+) provide isotope shifts of other bands that are not assigned to this system. The solid line is drawn with the theoretically predicted slope of −0.002 86 as a guide for the eye.

In any case, it appears that these bands belong to the same band system. In accord with the assignment of the 23 849 cm^{-1} feature as the origin band, this upper state is designated as the $[23.8]\Omega=0^+$ state. Because of the erratic nature of the upper state intervals and rotational constants, it seems unreasonable to extract vibrational $(\omega_e, \omega_e x_e)$ or rotational (B_e, α_e) constants for this electronic state. In contrast, the ground state seems to be unperturbed, and data from this band system may be combined with data from the other band systems described below to obtain accurate values of $\Delta G_{1/2}$, $\Delta G_{3/2}$, ω''_e, $\omega''_e x''_e$, B''_e, α''_e, and r''_e. These results are described in the next subsection, where bands originating from $v''=1$ and 2 have been rotationally resolved.

D. The $[24.2]\Omega=0^+$ state

Also shown in Table I are the spectroscopic constants for five rotationally resolved bands that connect the ground state to an electronic state with an origin near 24 182 cm^{-1}. This is designated as the $[24.2]\Omega=0^+\leftarrow X\,^1\Sigma^+$ system. Initially it was found that the three bands designated as the 0–2, 0–1, and 0–0 bands yielded $(\nu, \Delta\nu)$ data pairs that fit well to a line of slope −0.002 792. This is, again, very close to the predicted value of −0.002 861. Such a close match is not expected for a progression in the upper state because of the

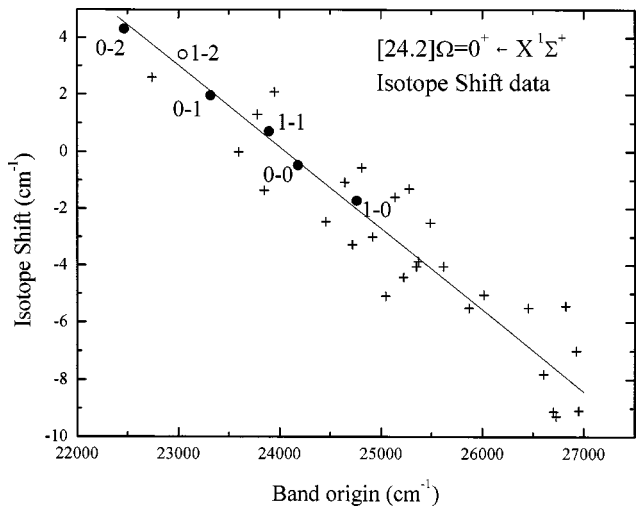

FIG. 4. Measured isotope shifts vs band origin. Bands assigned to the $[24.2]0^+ \leftarrow X\,^1\Sigma^+$ system are shown as circles, with solid circles providing isotope shifts measured in high resolution. Open circles provide isotope shifts measured from low resolution scans. Plus signs (+) provide isotope shifts of other bands that are not assigned to this system. The solid line is drawn with the theoretically predicted slope of −0.002 86 as a guide for the eye.

extensive perturbations that are typically present. The three bands near 22 464, 23 317, and 24 182 cm^{-1} must, therefore, be a progression in the ground state corresponding to different values of v''. This is confirmed by the values of $\Delta G''_{1/2}$ and $\Delta G''_{3/2}$, 864.3931(26) and 853.6288(50) cm^{-1}, respectively, obtained for this progression. The value of $\Delta G''_{1/2}$ determined for this system and that determined from the data for the $[23.8]\Omega=0$ system [864.4017(54) cm^{-1}] are identical to within experimental error. The agreement between the two values of $\Delta G''_{3/2}$ is somewhat less satisfying, but this is not surprising because the value calculated from the $[23.8]0^+ \leftarrow X\,^1\Sigma^+$ system is based on low-resolution data. The values of $\Delta G''_{1/2}$ and $\Delta G''_{3/2}$ obtained from all rotationally resolved scans may be averaged to obtain $\Delta G''_{1/2} = 864.3919(21)$ cm^{-1} and $\Delta G''_{3/2} = 853.6289(50)$ cm^{-1} for $^{58}Ni^{12}C$; $\Delta G''_{1/2} = 861.9526(23)$ cm^{-1} is obtained for $^{60}Ni^{12}C$. These values lead to $\omega_e = 875.155$ cm^{-1} and $\omega_e x_e = 5.382$ cm^{-1} for $^{58}Ni^{12}C$.

When the line with the theoretical slope of −0.002 861 is extended through the 0–2, 0–1, and 0–0 bands on the $(v, \Delta v)$, plot, two additional bands that were rotationally resolved are found to lie close to this line. These are the 1–1 and 1–0 bands of the $[24.2]\Omega=0^+ \leftarrow X\,^1\Sigma^+$ system, which are also listed in Table I. The corresponding $(v, \Delta v)$ plot is displayed in Fig. 4. Close examination of the low resolution spectrum also shows a weak feature near the expected position of the 1–2 band, with an isotope shift measured in low resolution that is consistent with expectations. Based on the assigned bands, a value of $\Delta G'_{1/2} = 578.914(9)$ is found for the $[24.2]\Omega=0^+ \leftarrow X\,^1\Sigma^+$ system. Due to perturbations, the B'_1 value is actually larger than the B'_0 value, making it meaningless to extract values of B_e, α_e, or r_e for this system.

E. The $[24.6]\Omega=0^+$ state

Another line of slope −0.002 753 can be drawn through $(v, \Delta v)$ data pairs for the bands near 23 780 and 24 644 cm^{-1}. The interval between these two bands is 863.64(50) cm^{-1}, a number that is close to the value of $\Delta G''_{1/2} = 864.3919(21)$ cm^{-1} calculated from a number of band pairs. These two bands must surely be the 0–1 and 0–0 bands of yet another band system. The isotope shift for the 0–0 band is roughly what can be expected for an origin band in this molecule. An attempt to use the 0–0 band to extrapolate a line of slope −0.002 86 to the blue yielded no candidates for the 1–0 band of this system, however.

F. The $[24.8]\Omega=0^+$ state

One more line can be drawn through the $(v, \Delta v)$ data pairs, allowing another band system to be located. The bands are located near 23 947 and 24 810 cm^{-1} and are assigned as the 0–1 and 0–0 bands of the $[24.8]\Omega=0^+ \leftarrow X\,^1\Sigma^+$ system. The interval calculated from these bands is 863.19(50) cm^{-1}, where the lack of precision again results from the fact that the 0–1 band was not examined in high resolution. The line connecting these bands can be extended to intersect another band about 676 cm^{-1} to the blue. This band, however, has an upper state rotational constant (0.5086 cm^{-1}) that is considerably larger than the upper state rotational constant for the 0–0 band (0.4747 cm^{-1}). In addition, the upper state lifetime of the candidate band is 93 ns, considerably shorter than the 214 ns lifetime of the upper state of the 0–0 band. It, therefore, seems unconvincing to assign this as the 1–0 band of the system. Presumably all of the upper states in this energy range are heavily perturbed, making the assignment of bands to band systems an exercise in futility. None of the remaining unclassified bands can be convincingly assigned as belonging to this band system.

G. Ionization energy

Observation of the 0–0 band of the $[21.7]0^+ \leftarrow X\,^1\Sigma^+$ system, the redmost band observed in this study, using ArF excimer radiation at 6.42 eV implies that the sum of the two photon energies is sufficient to ionize NiC from its ground level. This places the ionization energy of NiC below 9.12 eV. To establish a lower bound for the ionization energy, an attempt was made to record spectra using KrF excimer radiation (5.00 eV) for photoionization. However, even the highest frequency band observed, at 26 951 cm^{-1}, could not be detected using this ionization source. This implies that the ionization energy of NiC is greater than the sum of these two photon energies, placing IE(NiC) above 8.34 eV. Combining these upper and lower limits into a single statement, we obtain $8.34\ \text{eV} < \text{IE(NiC)} < 9.12\ \text{eV}$, or $\text{IE(NiC)} = 8.73 \pm 0.39$ eV. This value is considerably larger than the ionization energy of atomic nickel (7.637 eV).[77]

The thermodynamic cycle

TABLE III. Spectroscopic constants of the $X\,^1\Sigma^+$ ground state of NiC.[a]

Parameter	Value of parameter		
	$^{58}Ni^{12}C$	$^{60}Ni^{12}C$	$^{62}Ni^{12}C$
$\Delta G_{1/2}$ (cm^{-1})	864.3919(21)	861.9526(23) cm^{-1}	
$\Delta G_{3/2}$ (cm^{-1})	853.6289(50)		
ω_e (cm^{-1})	875.155		
$\omega_e x_e$ (cm^{-1})	5.382		
B_0 (cm^{-1})	0.637 648 33(14)[b]	0.634 014 58(20)[b]	0.630 31(57)
B_1 (cm^{-1})	0.632 31(17)	0.629 58(36)	
B_2 (cm^{-1})	0.624 93(88)		
B_e (cm^{-1})	0.640 38(14)	0.636 23(18)	
α_e (cm^{-1})	0.005 47(19)	0.004 44(36)	
r_e (Å)	1.627 29(17)	1.627 92(23)	
r_0 (Å)	1.630 773	1.630 761	1.631 14(74)
IE (eV)		8.73 ± 0.39	
D_0 (eV)		$\geqslant 3.34$ eV	

[a]Error limits are given in parentheses in units of the last reported digits, and represent 1σ in the fitted quantity.
[b]From Ref. 1.

$$\begin{array}{ccc} NiC & \xrightarrow{IE(NiC)} & NiC^+ \\ \Big\downarrow D_0(NiC) & & \Big\uparrow -D_0(Ni^+\text{-}C) \\ Ni + C & \xrightarrow{IE(Ni)} & Ni^+ + C \end{array} \qquad (3.6)$$

demonstrates that $D_0(\mathrm{NiC}) - D_0(\mathrm{Ni}^+ - \mathrm{C}) = \mathrm{IE(NiC)} - \mathrm{IE(Ni)}$. Hence, the fact that IE(NiC) exceeds IE(Ni) by 1.09 ± 0.39 eV implies that the bond dissociation energy of neutral NiC similarly exceeds that of NiC^+ by 1.09 ± 0.39 eV as well.

Finally, we note that our inability to observe spectroscopic transitions in NiC to the red of 21 748 cm^{-1} does not imply that the spectrum to the red of this limit is devoid of transitions. Given the high ionization energy of NiC, it is likely that additional band systems exist to the red of this wave number, but that the excited states reached in these transitions cannot be one-photon ionized by ArF excimer radiation at 6.42 eV. They are, therefore, invisible to the present investigation, but could probably be productively studied using other methods, such as laser-induced fluorescence spectroscopy.

IV. DISCUSSION

A. The NiC $X\,^1\Sigma^+$ ground state

The fact that every rotationally resolved band investigated in this study originates from the same $\Omega = 0$ electronic state convincingly demonstrates that the ground electronic state of NiC possesses $\Omega = 0$. Further, based on the agreement among all of the theoretical studies of this molecule, it may be assumed that this is a closed-shell state of $^1\Sigma^+$ symmetry.[65–68] Given that the isovalent molecules NiSi,[67,78,79] PdC,[6,7] PtC,[34,35,43] and PtSi[80] all have the analogous $^1\Sigma^+$ ground state, the fact that NiC shares this ground-state symmetry should not come as a surprise.

The experimentally determined properties of the NiC $X\,^1\Sigma^+$ ground state are summarized in Table III. The measured values of $r_e = 1.627$ Å and $\omega_e = 875.16\ cm^{-1}$ for $^{58}Ni^{12}C$ are in remarkably good agreement with the most recent *ab initio* calculation on this molecule by Shim and Gingerich, who use multireference configuration interaction (MRCI) calculations to obtain $r_e = 1.621$ Å and $\omega_e = 874\ cm^{-1}$.[68] Based on the quality of this agreement, one may conclude with confidence that modern methods of *ab initio* quantum chemistry are certainly capable of accurately describing the ground electronic state in molecules such as NiC. This is not at all trivial, because the $3d$ metals are notorious for presenting serious calculational difficulties due to the importance of electron correlation within the compact $3d$ subshell.

In addition to providing accurate values of r_e and ω_e, the calculation provides a means of understanding the chemical bonding in NiC, and allows the high ionization potential of NiC (compared to Ni) to be rationalized. According to Shim and Gingerich, the ground and low-lying electronic states of NiC derive from the separated ion limit Ni^+, $3d^8 4s^1$, $^4F + C^-$, $2s^2 2p^3$, $^4S^o$.[68] Thus, the ground state of the molecule has substantial ionic character, a fact that is reflected in the large dipole moment (2.358 D) calculated for the ground state. In contrast, NiC^+ undoubtedly dissociates to the $Ni^+ + C$ limit, which has no long range $-e^2/R$ Coulomb attraction. As a result, the bond energy of the NiC^+ cation is reduced compared to that of the NiC neutral molecule. The thermochemical cycle (3.6) then implies that the ionization energy of NiC is increased relative to that of atomic Ni as well. Our results indicate that the bond energy of NiC exceeds that of NiC^+ by 1.09 ± 0.39 eV, in agreement with this expectation. Similar, but much larger effects are typically observed in molecules that are more highly ionic, with the bond energy of NaCl, for example, exceeding that of $NaCl^+$ by more than 3.5 eV.[81] For other ionic molecules, such as NaBr, NaI, KCl, KBr the bond energy of the neutral molecule exceeds that of the molecular cation by 3.17, 2.5, 4.1, and 3.5 eV, respectively.[81]

Our observation of long-lived excited electronic states as far to the blue as 26 951 cm^{-1} strongly suggests that the

TABLE IV. Ground states of the transition metal carbides.[a]

Molecule	Ground-state configuration and term	Bond length (Å)	Vibrational frequency (cm^{-1})	Bond energy, D_e (eV)
ScC	$[7\sigma^2 3\pi^3 8\sigma^2,\ ^2\Pi_i]$[b]	$[r_e = 1.988$[b]$]$	[607[b]]	$< 4.56 \pm 0.22$;[c] [2.84[b]]
TiC	$[7\sigma^2 3\pi^4 8\sigma^1 9\sigma^1,\ ^3\Sigma^+]$[d,e,f,g]	$[r_e = 1.712$[g]$]$	[869[g]]	<4.48;[h] [3.52,[f] 3.57[g]]
VC	$7\sigma^2 3\pi^4 8\sigma^2 1\delta^1,\ ^2\Delta_r$[i,j,k]	$[r_e = 1.65$[k]$]$	[733[k]]	4.38 ± 0.25;[l] [2.9[k]]
CrC	$[7\sigma^2 3\pi^4 8\sigma^2 1\delta^2,\ ^3\Sigma^-]$[m,n]	$[r_e = 1.68$[n]$]$	[675[n]]	[2.98[n]]
MnC	$[7\sigma^2 3\pi^4 8\sigma^2 1\delta^2 9\sigma^1,\ ^4\Sigma^-]$[o]	No experiments, no calculations		
FeC	$7\sigma^2 3\pi^4 8\sigma^2 1\delta^3 9\sigma^1,\ ^3\Delta_i$[p]	$r_e = 1.58894$[q]	867.32[q]	$< 3.9 \pm 0.3$;[r] [2.79,[s] 3.53,[t] 3.76[u]]
CoC	$7\sigma^2 3\pi^4 8\sigma^2 1\delta^4 9\sigma^1,\ ^2\Sigma^+$[v]	$r_0 = 1.561217$[w]	947[x]	Unknown
NiC	$7\sigma^2 3\pi^4 8\sigma^2 1\delta^4 9\sigma^2,\ ^1\Sigma^+$[y]	$r_e = 1.6273$[z]	875.1[z]	$\geqslant 3.34$ eV;[z] [2.76[aa]]
CuC	$[7\sigma^2 3\pi^4 8\sigma^2 1\delta^4 9\sigma^2 4\pi^1,\ ^2\Pi_r]$[o]	No experiments, no calculations		
ZnC	$[7\sigma^2 3\pi^4 8\sigma^2 1\delta^4 9\sigma^2 4\pi^2,\ ^3\Sigma^-]$[bb]	$[r_e = 1.992$[bb]$]$	[482[bb]]	[0.923[bb]]

[a]Theoretical results are given in square brackets. Experimental results are given without brackets. Bond energies are given relative to the energy of the separated ground state atoms.
[b]Reference 51.
[c]Reference 95.
[d]Reference 52.
[e]Reference 53.
[f]Reference 54.
[g]Reference 55.
[h]Reference 96.
[i]Reference 92.
[j]Reference 56.
[k]Reference 57.
[l]Reference 97.
[m]Reference 59.
[n]Reference 60.
[o]See discussion in the text.
[p]References 3, 44–48, 62–64.
[q]Reference 48.
[r]Reference 3.
[s]Reference 62.
[t]Reference 63.
[u]Reference 64.
[v]References 1, 49, 50.
[w]Reference 1.
[x]Reference 49.
[y]References 1, 67, and 68.
[z]This work.
[aa]Reference 68.
[bb]Reference 94.

bond energy of NiC exceeds this value, which converts to 3.34 eV. In many molecules with a density of electronic states similar to that expected in NiC, we have found that predissociation sets in abruptly at a specific energy in the molecule, and all states lying above this energy dissociate on a rapid time scale. For example, in AlNi, which is expected to have a smaller density of electronic states than NiC, a sharp predissociation threshold has been observed at 19 836 cm^{-1}.[82] Based on our observation of long-lived vibronic levels up to 26 951 cm^{-1}, we assign $D_0(\mathrm{NiC}) \geqslant 3.34$ eV in Tables III and IV.

B. Chemical bonding trends in the ligated transition metals

1. Trends as the ligand is varied from C to N to O to F

In surveying the trends in electronic structure among the transition metal carbides, nitrides, oxides, and fluorides, the fact that the $2s$ and $2p$ orbitals of the ligand drop in energy as one moves from C to N to O to F exerts a powerful influence on the electronic structure of the molecule. The $2s$ and $2p$ orbital energies of these atoms, obtained by numerical Hartree–Fock[83] calculations on the ground terms arising from the $1s^2 2s^2 2p^n$ ground configurations, are plotted in Fig. 5, along with horizontal lines that provide the orbital energies of the $3d$ and $4s$ orbitals of Ni, calculated for the $3d^9 4s^1$, ^{3}D state. It is evident that the $2s$ orbital rapidly becomes irrelevant for chemical bonding as it drops to extremely low energies. Further, as the $2p$ orbitals drop in energy relative to the metal $3d$ and $4s$ orbitals, there is less mixing between the ligand orbitals and the metal orbitals, and the system becomes dominated by electron transfer from the metal atom to the ligand. In simple terms, the bonding becomes more ionic in character as one moves to more electronegative ligands.

The disparity between the metal and ligand orbital energies that develops as one moves to more electronegative ligands also leads to smaller orbital splitting patterns in the metal-based orbitals for the more electronegative ligands. This is illustrated in the qualitative molecular orbital diagrams displayed in Fig. 6 for FeC, FeN, and FeF. As the ligand $2p$ orbitals drop lower in energy, they become more energetically removed from the metal orbitals, causing the splitting of the metal-based orbitals to decrease. A general result of this effect is that transition metals bonded to more electronegative ligands (such as F) tend to form high-spin molecules, in which several unpaired electrons are placed in different metal-centered orbitals. For the more covalently bound transition metal carbides, the larger splitting among the metal-centered orbitals leads to a preference for low-spin ground states. Thus, for example, one finds that the series of ligated iron compounds have ground states of $1\delta^3 9\sigma^1$, $^3\Delta_i$ for FeC;[3,44–46] $1\delta^3 9\sigma^1 4\pi^1$, $^4\Pi_i$ for FeN;[84] $1\delta^3 9\sigma^1 4\pi^2$, $^5\Delta_i$ for FeO;[85] and $1\delta^3 9\sigma^1 4\pi^2 10\sigma^1$, $^6\Delta_i$ for FeF.[86,87] Similarly, if one examines a set of isovalent metal–ligand compounds such as NiC, CoN, FeO, and MnF, one finds ground states of $1\delta^4 9\sigma^2$, $^1\Sigma^+$ for NiC;[1] $1\delta^3 9\sigma^1 4\pi^2$, $^5\Delta$ for CoN (from a density functional calculation);[88] $1\delta^3 9\sigma^1 4\pi^2$, $^5\Delta$ for FeO;[85] and $1\delta^2 9\sigma^1 4\pi^2 10\sigma^1$, $^7\Sigma^+$ for MnF.[89,90] This pattern of increasing spin multiplicity as one moves to more electronegative ligands is a natural consequence of the fact that the $2p$ orbitals drop as one moves across the C, N, O, F sequence. For molecules that have not yet been examined either spectroscopically or by theory, this pattern of increas-

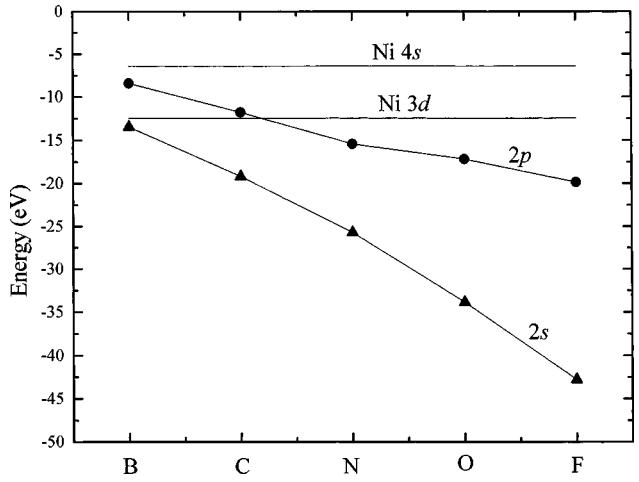

FIG. 5. Orbital energies of the $2s$ and $2p$ atomic orbitals of B, C, N, O, and F, calculated by numerical Hartree–Fock methods, compared to the corresponding orbital energies of the $3d$ and $4s$ orbitals of nickel.

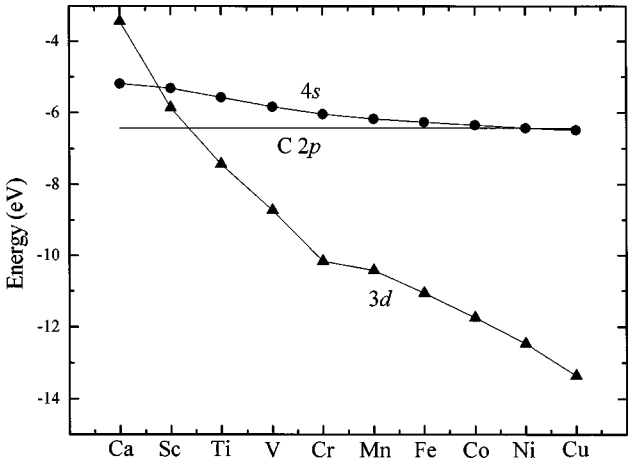

FIG. 7. Orbital energies of the $3d$ and $4s$ orbitals of the $3d$ series of metal atoms, calculated by numerical Hartree–Fock methods for the high-spin $3d^n4s^1$ configurations of the metals. Although both atomic orbitals drop in energy with increasing atomic number, the magnitude of this drop is much greater for the $3d$ orbitals. The horizontal line gives the Hartree–Fock energy of the $2p$ orbital of carbon, for comparison.

ing spin multiplicity provides a useful means of guessing the symmetry of the ground electronic state.

2. Trends as the transition metal is varied

In addition to the systematic effects that are observed as the ligand is varied, some general trends are evident in the chemical bonding as one examines the ground states of the various transition metal carbides. A major factor that effects the electronic structure of these species is the energy of the $3d$ and $4s$ atomic orbitals, as they compare to the energy of the carbon $2p$ orbital and to each other. The trends in these orbital energies, as calculated by numerical Hartree–Fock methods for the $3d^n4s^1$ configurations,[83] are displayed in Fig. 7 for the atoms Ca through Cu. The figure demonstrates that as the nuclear charge on the atom increases, the orbital energies drop for both the $3d$ and the $4s$ orbitals. However, the magnitude of the drop in orbital energy is much greater for the $3d$ than for the $4s$ orbitals. Thus, at the beginning of the series, the $4s$ orbital is preferentially occupied, but the $3d$ orbitals drop rapidly in energy so that they are soon the orbitals that are preferentially occupied, ultimately becoming corelike in Cu and Zn. Although Fig. 7 is useful, it is important to realize that the orbital energies change when the atom adopts a different electronic configuration, and a somewhat different diagram would have been obtained if we had chosen to plot the orbital energies taken from the $3d^{n-1}4s^2$ configuration instead of the $3d^n4s^1$ configuration.

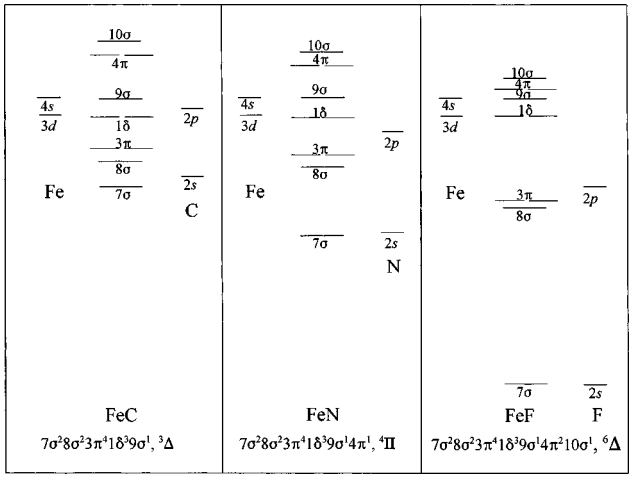

FIG. 6. Qualitative molecular orbital diagrams for FeC, FeN, and FeF. These diagrams display the effect that a more electronegative ligand has on the molecular orbital structure of the system. In general, the more electronegative the ligand, the smaller the splitting among the metal-based orbitals. This phenomenon leads to high multiplicity ground states in the metal fluorides, and lower multiplicity ground states in the metal carbides.

Considering the interactions between the valence $2s$ and $2p$ orbitals of carbon and the valence $3d$ and $4s$ orbitals of the metal leads to molecular orbitals consisting of the 7σ, 8σ, 9σ, and 10σ; the 3π and 4π; and the 1δ orbitals. The 7σ orbital is thought to be primarily carbon $2s$ in character. Although it is certainly relevant to the electronic structure of the molecule, it is almost corelike in character and is filled in all of the transition metal carbides. The 8σ orbital is a bonding combination of the metal $3d\sigma$ and carbon $2p\sigma$ orbitals, with a small amount of $4s\sigma$ character as well. The 9σ orbital is primarily nonbonding in character, and is mainly made up of the metal $4s\sigma$ orbital. Some metal $4p\sigma$ character may be mixed in as well, allowing this orbital to polarize away from the negatively charged carbon atom. Finally, the 10σ orbital is the antibonding analog of the 8σ orbital, composed mainly of metal $3d\sigma$ and carbon $2p\sigma$ character. Among the π orbitals, the 3π is a bonding combination of the metal $3d\pi$ and carbon $2p\pi$ atomic orbitals, and the 4π is the corresponding antibonding combination. Finally, the nonbonding 1δ orbital is almost entirely composed of metal $3d$ character. As such, its energy follows the trend with increasing nuclear charge that is illustrated in Fig. 7 for the $3d$ orbitals. This general description of the molecular orbitals is valid for metals near the center of the $3d$ series, but it may require modification for the early transition metal carbides, such as ScC, particularly as regards the atomic character of the σ orbitals.

Although there is little experimental information about many of the $3d$ transition metal carbides, the available theoretical and experimental work (summarized in Table IV) demonstrates that the pattern of $3d$ versus $4s$ energy displayed in Fig. 7 is paralleled by the relative energies of the 1δ orbital (which is almost exclusively $3d$ in character) and the 9σ orbital (which is primarily $4s$ in character). Thus, in the early transition metal carbides ScC[51] and TiC,[52–55] calculations predict that the $4s$-like σ orbital holds one or two electrons while the $3d$-like 1δ orbital is empty. This is in accord with Fig. 7, where the $4s$ orbital is most favored for the metals with the smallest nuclear charge. (It should be noted that in the case of ScC, it is the 8σ orbital that is thought to have substantial $4s$ character on scandium.)[51]

The situation changes with VC, for which the ground state is $7\sigma^2 8\sigma^2 3\pi^4 1\delta^1$, $^2\Delta_r$.[56,57,91,92] Now it is the 1δ orbital that is occupied by one electron and the $4s$-like 9σ orbital that is empty. Likewise, CrC is calculated to have a $7\sigma^2 8\sigma^2 3\pi^4 1\delta^2$, $^3\Sigma^-$ ground state that leaves the 9σ orbital empty.[59,60] Interestingly, the calculated ground states of ScC, TiC, and VC all correlate to their respective ground state separated atom limits. The calculated $7\sigma^2 8\sigma^2 3\pi^4 1\delta^2$, $^3\Sigma^-$ ground state of CrC, however, cannot dissociate to the ground state separated atom limit of Cr, $3d^5 4s^1$, ^{7}S+C, $2s^2 2p^2$, ^{3}P, because this limit only generates states with total electron spin of S=2, 3, or 4 (2S+1=5, 7, or 9). The calculated $X\,^3\Sigma^-$ ground state instead dissociates to the excited separated atom limit of Cr, $3d^5 4s^1$, ^{5}S+C, $2s^2 2p^2$, ^{3}P, which lies 0.94 eV above ground-state atoms.[93] In addition, the $X\,^3\Sigma^-$ ground state probably has a significant contribution from the Cr^+, $3d^5$, ^{6}S+C^-, $2p^3$, $^4S^o$ ion pair limit, which also generates a $^3\Sigma^-$ state. In any case, the bond energy of CrC is significantly weakened by the 0.94 eV promotion energy that is required to prepare the Cr atom for bonding.

Currently, no theoretical or experimental work exists on MnC, but given the tremendous exchange stabilization of the high-spin ground state of atomic manganese ($3d^5 4s^2$, ^{6}S), it is extremely likely that the 9σ orbital is now occupied to give a $7\sigma^2 8\sigma^2 3\pi^4 1\delta^2 9\sigma^1$, $^4\Sigma^-$ ground state. This is the lowest multiplicity state that can correlate to ground-state atoms (Mn, $3d^5 4s^2$, ^{6}S+C, $2s^2 2p^2$, ^{3}P). Indeed, the lowest separated atom limit that can produce a doublet state (such as the $7\sigma^2 8\sigma^2 3\pi^4 1\delta^3$, $^2\Delta_i$ state) is Mn, $3d^6 4s^1$, ^{4}D+C, $2s^2 2p^2$, ^{3}P, which lies 2.89 eV above ground state atoms.[93] This is far too high in energy to correlate to the ground state of the molecule. Even if one considers the molecule to derive from the Mn^+, $3d^5 4s^1$, ^{7}S+C^-, $2s^2 2p^3$, $^4S^o$ ionic limit, simple electron pairing considerations again demand that the system will have a $7\sigma^2 8\sigma^2 3\pi^4 1\delta^2 9\sigma^1$, $^4\Sigma^-$ ground state. Despite the fact that neither calculations nor experiments have been performed on this molecule, it seems virtually certain that MnC has a $^4\Sigma^-$ ground state.

The next transition metal carbide, FeC, has been well-characterized both experimentally[3,44–48] and theoretically.[62–64] The ground state is $7\sigma^2 8\sigma^2 3\pi^4 1\delta^3 9\sigma^1$, $^3\Delta_i$, which seems to contradict the expectations that are set up by the orbital energy diagram shown in Fig. 7. By the time one reaches Fe, the orbital energy of the $3d$ orbitals lies far below that of the $4s$ orbital, so one might expect the ground state to place four electrons in the $3d$-like 1δ orbital, giving a $7\sigma^2 8\sigma^2 3\pi^4 1\delta^4$, $^1\Sigma^+$ state. However, the low-spin $^1\Sigma^+$ state cannot correlate to the ground separated atom limit of Fe, $3d^6 4s^2$, ^{5}D+C, $2s^2 2p^2$, ^{3}P, because this limit generates no singlet states. The lowest state of the neutral separated atoms that can correlate to a $^1\Sigma^+$ state is the Fe, $3d^7 4s^1$, ^{3}F+C, $2s^2 2p^2$, ^{3}P separated atom asymptote at 1.49 eV.[93] This is a high promotion energy price that must be paid in order to attain a closed shell $^1\Sigma^+$ ground state, particularly because the 1δ orbital offers no significant bonding advantage over the nonbonding 9σ orbital. In the isovalent RuC molecule, $^1\Sigma^+$ does emerge as the ground state (barely, since $^3\Delta_3$ lies only 75 cm^{-1} higher in energy),[5] but for this system the lowest spin–orbit component of the analogous Ru, $4d^7 5s^1$, ^{3}F+C, $2s^2 2p^2$, ^{3}P separated atom asymptote lies only 0.81 eV above the ground state separated atoms.[93] Thus, in RuC the promotion energy required to prepare the system for bonding in the closed-shell, $^1\Sigma^+$ state is only 0.81 eV, compared to 1.49 eV for FeC. As a result, these isovalent molecules have different ground electronic states.

Moving on to CoC, we find that the next electron enters the 1δ orbital to give a $7\sigma^2 8\sigma^2 3\pi^4 1\delta^4 9\sigma^1$, $^2\Sigma^+$ ground state that has been experimentally well-characterized.[1,49,50] One of the more interesting aspects about this molecule is that hyperfine measurements have established that the 9σ orbital has ~89% cobalt $4s$ character.[49] Thus, when one reaches CoC, the $3d$-like 1δ orbital is completely filled and the $4s$-like 9σ orbital is half-filled. This agrees with the expectations one might have based on the orbital energies of the $3d$ versus $4s$ atomic orbitals, as displayed in Fig. 7.

Finally, previous theoretical[65–68] and experimental work,[1] along with the present study, demonstrate that NiC has a $7\sigma^2 8\sigma^2 3\pi^4 1\delta^4 9\sigma^2$, $^1\Sigma^+$ ground state. With Cu and Zn, the antibonding 4π orbitals are expected to begin filling, giving ground states of $7\sigma^2 8\sigma^2 3\pi^4 1\delta^4 9\sigma^2 4\pi^1$, $^2\Pi_r$ and $7\sigma^2 8\sigma^2 3\pi^4 1\delta^4 9\sigma^2 4\pi^2$, $^3\Sigma^-$ for CuC and ZnC, respectively.[94] For all three molecules, NiC, CuC, and ZnC, the known or expected ground state derives from the ground separated atom limit, and no promotion energy is required to prepare the atoms for bonding. Nevertheless, the bond energy is expected to drop in moving from NiC to CuC due to the reduced ability of Cu to engage in π-bonding, and to drop precipitously in moving from CuC to ZnC. In ZnC the bond is formed by donation of the Zn $4s$ electron pair into an empty $2p\sigma$ orbital of carbon, leaving the two $2p$ electrons on carbon in the $2p\pi$ orbitals, high-spin coupled to form a $^3\Sigma^-$ ground state.[94] In essence, ZnC is bound by a Lewis acid—Lewis base interaction, much the same as in the classic BF_3 complex with NH_3. These expectations of a weakened chemical bond as one moves from NiC to CuC and on to ZnC are in accord with our lower limit of $D_0(\mathrm{NiC}) \geqslant 3.34$ eV and the calculated bond energy of $D_e(\mathrm{ZnC}) = 0.923$ eV.[94]

V. CONCLUSIONS

Optical spectra of diatomic NiC have been recorded in the range from 19 200 to 27 000 cm^{-1}, allowing the ground state of this molecule to be understood in greater detail.

Spectroscopic parameters of $\omega_e = 875.155\ \mathrm{cm}^{-1}$, $\omega_e x_e = 5.382\ \mathrm{cm}^{-1}$, $B_e = 0.640\,38(14)\ \mathrm{cm}^{-1}$, $\alpha_e = 0.004\,44(36)\ \mathrm{cm}^{-1}$, and $r_e = 1.627\,29(17)$ Å are obtained for $^{58}Ni^{12}C$ in its $7\sigma^2 8\sigma^2 3\pi^4 1\delta^4 9\sigma^2$, $^1\Sigma^+$ ground state. The observation of long-lived vibronic states at high energies also strongly suggests that $D_0(\mathrm{NiC}) \geqslant 3.34$ eV. The ionization energy of the molecule has been determined to fall within the limits $\mathrm{IE(NiC)} = 8.73 \pm 0.39$ eV.

In general, the excited electronic states of NiC display a complicated pattern of vibronic levels due to extensive perturbations among the $\Omega = 0^+$ excited states. Nevertheless, several vibronic levels have been classified into band systems. In general, the states probed in the 23 800–27 000 cm^{-1} range display a large increase in bond length relative to the ground state, and these states have short lifetimes (100–300 ns). One excited electronic state stands out as being rather isolated from other band systems. It is the $[21.7]\Omega = 0^+$ state, with $T_0 = 21\,748.69\ \mathrm{cm}^{-1}$ and $r_0 = 1.6476$ Å, $\tau = 560 \pm 65$ ns.

ACKNOWLEDGMENTS

We thank the U.S. Department of Energy (DE-FG03-01ER15176) for support of this research. The authors would also like to heartily thank Professor Tim Steimle for his gift of the isotopically pure ^{130}Te and sealed absorption cell used to calibrate the rotationally resolved spectra collected in the range from 20 000 to 23 800 cm^{-1}. Without this generosity, this study would have been much more difficult to complete.

[1] M. A. Brewster and L. M. Ziurys, Astrophys. J. Lett. **559**, L163 (2001).
[2] G. von Helden, A. G. Tielens, D. van Heijnsbergen, M. A. Duncan, S. Hony, L. B. Waters, and G. Meijer, Science **288**, 313 (2000).
[3] D. J. Brugh and M. D. Morse, J. Chem. Phys. **107**, 9772 (1997).
[4] D. J. Brugh, T. J. Ronningen, and M. D. Morse, J. Chem. Phys. **109**, 7851 (1998).
[5] J. D. Langenberg, R. S. DaBell, L. Shao, D. Dreessen, and M. D. Morse, J. Chem. Phys. **109**, 7863 (1998).
[6] J. D. Langenberg, L. Shao, and M. D. Morse, J. Chem. Phys. **111**, 4077 (1999).
[7] R. S. DaBell, R. G. Meyer, and M. D. Morse, J. Chem. Phys. **114**, 2938 (2001).
[8] S. M. Sickafoose, A. W. Smith, and M. D. Morse, J. Chem. Phys. **116**, 993 (2002).
[9] B. Simard, P. A. Hackett, and W. J. Balfour, Chem. Phys. Lett. **230**, 103 (1994).
[10] A. J. Merer and J. R. D. Peers, in *Ohio State 53rd International Symposium on Molecular Spectroscopy* (Columbus, OH, 1998), abstract RI04 and 249.
[11] B. Simard, P. I. Presunka, H. P. Loock, A. Bérces, and O. Launila, J. Chem. Phys. **107**, 307 (1997).
[12] A. Lagerqvist, H. Neuhaus, and R. Scullman, Z. Naturforsch. **20a**, 751 (1965).
[13] A. Lagerqvist and R. Scullman, Ark. Fys. **32**, 475 (1966).
[14] B. Kaving and R. Scullman, J. Mol. Spectrosc. **32**, 475 (1969).
[15] W. J. Balfour, S. G. Fougère, R. F. Heuff, C. X. W. Qian, and C. Zhou, J. Mol. Spectrosc. **198**, 393 (1999).
[16] I. Shim, M. Pelino, and K. A. Gingerich, J. Chem. Phys. **97**, 9240 (1992).
[17] I. Shim and K. A. Gingerich, J. Chem. Phys. **106**, 8093 (1997).
[18] P. Jackson, G. E. Gadd, D. W. Mackey, H. van der Wall, and G. D. Willett, J. Phys. Chem. A **102**, 8941 (1998).
[19] I. Shim, H. C. Finkbeiner, and K. A. Gingerich, J. Phys. Chem. **91**, 3171 (1987).
[20] I. Shim and K. A. Gingerich, Chem. Phys. Lett. **317**, 338 (2000).
[21] I. Shim and K. A. Gingerich, J. Chem. Phys. **81**, 5937 (1984).
[22] H. Tan, M. Liao, and K. Balasubramanian, Chem. Phys. Lett. **280**, 423 (1997).
[23] I. Shim and K. A. Gingerich, J. Chem. Phys. **76**, 3833 (1982).
[24] G. Pacchioni, J. Koutecký, and P. Fantucci, Chem. Phys. Lett. **92**, 486 (1982).
[25] I. Shim and K. A. Gingerich, Surf. Sci. **156**, 623 (1985).
[26] H. Tan, D. Dai, and K. Balasubramanian, Chem. Phys. Lett. **286**, 375 (1998).
[27] I. Shim and K. A. Gingerich, Chem. Phys. Chem. **2**, 125 (2001).
[28] X. Li, S. S. Liu, W. Chen, and L.-S. Wang, J. Chem. Phys. **111**, 2464 (1999).
[29] K. Jansson, R. Scullman, and B. Yttermo, Chem. Phys. Lett. **4**, 188 (1969).
[30] K. Jansson and R. Scullman, J. Mol. Spectrosc. **36**, 248 (1970).
[31] H. Neuhaus, R. Scullman, and B. Yttermo, Z. Naturforsch. **20a**, 162 (1965).
[32] R. Scullman and B. Yttermo, Ark. Fys. **33**, 231 (1966).
[33] O. Appelblad, R. F. Barrow, and R. Scullman, Proc. Phys. Soc., London **91**, 260 (1967).
[34] O. Appelblad, C. Nilsson, and R. Scullman, Phys. Scr. **7**, 65 (1973).
[35] T. C. Steimle, K. Y. Jung, and B.-Z. Li, J. Chem. Phys. **102**, 5937 (1995).
[36] T. C. Steimle, K. Y. Jung, and B.-Z. Li, J. Chem. Phys. **103**, 1767 (1995).
[37] S. A. Beaton and T. C. Steimle, J. Chem. Phys. **111**, 10876 (1999).
[38] T. C. Steimle, M. L. Costen, G. E. Hall, and T. J. Sears, Chem. Phys. Lett. **319**, 363 (2000).
[39] D. Majumdar and K. Balasubramanian, Chem. Phys. Lett. **284**, 273 (1998).
[40] K. Balasubramanian, J. Chem. Phys. **112**, 7425 (2000).
[41] G. Meloni, L. M. Thomson, and K. A. Gingerich, J. Chem. Phys. **115**, 4496 (2001).
[42] H. Tan, M. Liao, and K. Balasubramanian, Chem. Phys. Lett. **280**, 219 (1997).
[43] B. F. Minaev, Phys. Chem. Chem. Phys. **2**, 2851 (2000).
[44] W. J. Balfour, J. Cao, C. V. V. Prasad, and C. X. Qian, J. Chem. Phys. **103**, 4046 (1995).
[45] M. D. Allen, T. C. Pesch, and L. M. Ziurys, Astrophys. J. Lett. **472**, L57 (1996).
[46] K. Aiuchi, K. Tsuji, and K. Shibuya, Chem. Phys. Lett. **309**, 229 (1999).
[47] K. Aiuchi and K. Shibuya, J. Mol. Spectrosc. **209**, 92 (2001).
[48] M. Fujitake, A. Toba, M. Mori, F. Miyazawa, N. Ohashi, K. Aiuchi, and K. Shibuya, J. Mol. Spectrosc. **208**, 253 (2001).
[49] M. Barnes, A. J. Merer, and G. F. Metha, J. Chem. Phys. **103**, 8360 (1995).
[50] A. G. Adam and J. R. D. Peers, J. Mol. Spectrosc. **181**, 24 (1997).
[51] A. Kalemos, A. Mavridis, and J. F. Harrison, J. Phys. Chem. A **105**, 755 (2001).
[52] C. W. Bauschlicher, Jr. and P. E. M. Siegbahn, Chem. Phys. Lett. **104**, 331 (1984).
[53] M. D. Hack, R. G. A. R. Maclagan, G. E. Scuseria, and M. S. Gordon, J. Chem. Phys. **104**, 6628 (1996).
[54] S. Sokolova and A. Lüchow, Chem. Phys. Lett. **320**, 421 (2000).
[55] A. Kalemos and A. Mavridis, J. Phys. Chem. A **106**, 3905 (2002).
[56] S. M. Mattar, J. Phys. Chem. **97**, 3171 (1993).
[57] R. G. A. R. Maclagan and G. E. Scuseria, Chem. Phys. Lett. **262**, 87 (1996).
[58] I. Shim and K. A. Gingerich, Int. J. Quantum Chem., Quantum Chem. Symp. **23**, 409 (1989).
[59] I. Shim and K. A. Gingerich, Int. J. Quantum Chem. **42**, 349 (1992).
[60] R. G. A. R. Maclagan and G. E. Scuseria, J. Chem. Phys. **106**, 1491 (1997).
[61] B. K. Nash, B. K. Rao, and P. Jena, J. Chem. Phys. **105**, 11020 (1996).
[62] I. Shim and K. A. Gingerich, Eur. Phys. J. D **7**, 163 (1999).
[63] S. S. Itono, T. Taketsugu, T. Hirano, and U. Nagashima, J. Chem. Phys. **115**, 11213 (2001).
[64] D. Tzeli and A. Mavridis, J. Chem. Phys. **116**, 4901 (2002).
[65] K. Kitaura, K. Morokuma, and I. G. Csizmadia, THEOCHEM **5**, 119 (1982).
[66] I. Panas, J. Schule, U. Brandemark, P. Siegbahn, and U. Wahlgren, J. Phys. Chem. **92**, 3079 (1988).
[67] I. Shim and K. A. Gingerich, Z. Phys. D: At., Mol. Clusters **12**, 373 (1989).
[68] I. Shim and K. A. Gingerich, Chem. Phys. Lett. **303**, 87 (1999).
[69] W. J. Balfour (personal communication), 1997.
[70] Z. Fu, G. W. Lemire, Y. M. Hamrick, S. Taylor, J.-C. Shui, and M. D. Morse, J. Chem. Phys. **88**, 3524 (1988).
[71] J. Cariou and P. Luc, *Atlas du Spectre d'Absorption de la Molécule de*

Tellure entre 18 500–23 800 cm^{-1} (CNRS, Paris, 1980).
[72] J. Cariou and P. Luc, *Atlas du Spectre d'Absorption de la Molécule de Tellure, Partie 5: 21 100–23 800 cm^{-1}* (CNRS, Paris, 1980).
[73] S. Gerstenkorn, J. Verges, and J. Chevillard, *Atlas du Spectre d'Absorption de la Molécule d'Iode entre 11 000–14 000 cm^{-1}* (CNRS, Paris, 1982).
[74] G. Herzberg, *Molecular Spectra and Molecular Structure I. Spectra of Diatomic Molecules*, 2nd ed. (Van Nostrand Reinhold, New York, 1950).
[75] P. DeBièrre, M. Gallet, N. E. Holden, and I. L. Barnes, J. Phys. Chem. Ref. Data **13**, 809 (1984).
[76] See EPAPS Document No. E-JCPSA6-117-020246 for 32 pages of absolute line positions and rotational fits. A direct link to this document may be found in the online article's HTML reference section. The document may also be reached via the EPAPS homepage (http://www.aip.org/pubservs/epaps.html) or from ftp.aip.org in the directory /epaps/. See the EPAPS homepage for more information.
[77] C. Corliss and J. Sugar, J. Phys. Chem. Ref. Data **10**, 197 (1981).
[78] I. Shim and K. A. Gingerich, Z. Phys. D: At., Mol. Clusters **16**, 141 (1990).
[79] N. F. Lindholm, D. J. Brugh, G. K. Rothschopf, S. M. Sickafoose, and M. D. Morse, J. Chem. Phys. (to be published).
[80] L. Shao, S. M. Sickafoose, J. D. Langenberg, D. J. Brugh, and M. D. Morse, J. Chem. Phys. **112**, 4118 (2000).
[81] K. P. Huber and G. Herzberg, *Constants of Diatomic Molecules* (Van Nostrand Reinhold, New York, 1979).
[82] J. M. Behm, C. A. Arrington, and M. D. Morse, J. Chem. Phys. **99**, 6409 (1993).
[83] C. F. Fischer, *The Hartree–Fock Method for Atoms* (Wiley, New York, 1977).
[84] K. Aiuchi and K. Shibuya, J. Mol. Spectrosc. **204**, 235 (2000).
[85] M. D. Allen, L. M. Ziurys, and J. M. Brown, Chem. Phys. Lett. **257**, 130 (1996).
[86] M. D. Allen and L. M. Ziurys, Astrophys. J. **470**, 1237 (1996).
[87] M. D. Allen and L. M. Ziurys, J. Chem. Phys. **106**, 3494 (1997).
[88] L. Andrews, A. Citra, G. V. Chertihin, W. D. Bare, and M. Neurock, J. Phys. Chem. A **102**, 2561 (1998).
[89] T. C. DeVore, R. J. Van Zee, and W. Weltner, Jr., J. Chem. Phys. **68**, 3522 (1978).
[90] O. Launila, B. Simard, and A. M. James, J. Mol. Spectrosc. **159**, 161 (1993).
[91] R. J. Van Zee, J. J. Bianchini, and W. Weltner, Jr., Chem. Phys. Lett. **127**, 314 (1986).
[92] Y. M. Hamrick and W. Weltner, Jr., J. Chem. Phys. **94**, 3371 (1991).
[93] C. E. Moore, *Atomic Energy Levels*, Natl. Bur. Stand. U.S. Circ. No. 467 ed. (U.S. Government Printing Office, Washington, D.C., 1971).
[94] A. I. Boldyrev and J. Simons, Mol. Phys. **92**, 365 (1997).
[95] R. Haque and K. A. Gingerich, J. Chem. Phys. **74**, 6407 (1981).
[96] F. J. Kohl and C. A. Stearns, High. Temp. Sci. **6**, 284 (1974).
[97] S. K. Gupta and K. A. Gingerich, J. Chem. Phys. **74**, 3584 (1981).